Extrinsic Spin Nernst Effect from First Principles

Katarina Tauber,[1,2,*] Martin Gradhand,[3] Dmitry V. Fedorov,[1,2] and Ingrid Mertig[1,2]

[1]*Max Planck Institute of Microstructure Physics, Weinberg 2, 06120 Halle, Germany*
[2]*Institute of Physics, Martin Luther University Halle-Wittenberg, 06099 Halle, Germany*
[3]*H. H. Wills Physics Laboratory, University of Bristol, Bristol BS8 1TH, United Kingdom*

(Received 24 November 2011; published 10 July 2012)

We present an *ab initio* description of the thermal transport phenomenon called the spin Nernst effect. It refers to generation of a spin accumulation or a pure spin current transverse to an applied temperature gradient. This is similar to the intensively studied spin Hall effect described by intrinsic and extrinsic mechanisms due to an applied electric field. Analogously, several contributions are present for the spin Nernst effect. Here we investigate the extrinsic skew scattering mechanism which is dominant in the limit of dilute alloys. Our calculations are based on a fully relativistic Korringa-Kohn-Rostoker method and a solution of the linearized Boltzmann equation. As a first application, we consider a Cu host with Au, Ti, and Bi impurities.

DOI: 10.1103/PhysRevLett.109.026601 PACS numbers: 72.25.Ba, 71.15.Rf, 72.15.Jf, 85.75.−d

The possibility of pure spin current generation in nonmagnetic materials opens the opportunity for the practical realization of spintronic devices. The necessary spin currents can be created by the spin Hall effect (SHE) [1,2], which has been intensively studied during the last decade. Recently, a new field ''spin caloritronics'' [3] has arisen, which relates the spin degree of freedom to temperature gradients. By analogy with the SHE, where the transverse spin current is generated by an electric field, the spin current can be caused by a temperature gradient. This phenomenon is called the spin Nernst effect (SNE) [4,5]. This point becomes evident from Fig. 1 comparing the different effects in the same family as there are the conventional Hall and Nernst effects as well as the anomalous Hall effect (AHE) and the anomalous Nernst effect (ANE) [6]. We should mention that in Ref. [7] the same effect was studied for a Rashba-type model, but called thermo-spin Hall effect. However, following the settled nomenclature [4–6], we state that spin Nernst effect is the appropriate name for the discussed phenomenon.

Recently, another thermal phenomenon called spin Seebeck effect (SSE) attracted a lot of interest [8–11]. The effect refers to the generation of a spin-motive force in a ferromagnetic strip by an applied temperature gradient. It was detected as a linearly varying transverse voltage in normal metal contacts via the inverse SHE [8]. Originally, the difference of the spin-dependent Seebeck coefficients was used for an explanation [9]. However, after the effect was even observed in magnetic insulators and semiconductors [10,11], it was finally attributed to magnons [12]. In addition, an important influence of the substrate on the thermal transport was shown [13]. Nevertheless, the concept of the spin-dependent Seebeck coefficients is still useful for a description of thermally driven spin injection from a ferromagnet to a nonmagnetic material [14]. A detailed discussion of both types of experiment is given in Ref. [15].

In this Letter, we concentrate on the SNE caused by spin-dependent scattering of electrons at substitutional impurities in an ideal crystal. This extrinsic contribution provided by the skew scattering mechanism we calculate for Au, Ti, and Bi impurities in a Cu host. The electronic structure of the considered materials is obtained by a fully relativistic Korringa-Kohn-Rostoker method [16]. The transport properties are calculated within the semiclassical approach solving the linearized Boltzmann equation [17]. Recently, a similar formalism was successfully applied to the *ab initio* study of the skew scattering contribution of the SHE [18–21].

We consider two possible situations for an experimental observation of the SNE. One of them is related to the transverse spin accumulation near the two edges of the sample, which is equivalent to the first detection of the SHE [22]. Another one is connected with the creation of the transverse spin current and its detection using, for instance, the inverse spin Hall effect [23].

Let us start with the theoretical description of the effect within a two-current model neglecting spin-flip processes. The charge-current density $\boldsymbol{j}$ and the spin-current density $\boldsymbol{j}^s$ are given by

$$\boldsymbol{j} = \boldsymbol{j}^{\uparrow} + \boldsymbol{j}^{\downarrow}, \qquad \boldsymbol{j}^s = \boldsymbol{j}^{\uparrow} - \boldsymbol{j}^{\downarrow}, \tag{1}$$

where the partial current density $\boldsymbol{j}^{\uparrow}$ for spin-up electrons (spin-down electrons analogously) is defined by the linear response transport equation

	H≠0 M=0	H=0 M≠0	H=0 M=0
$\vec{E}$	Hall effect	AHE	SHE
∇T	Nernst effect	ANE	SNE

FIG. 1. The family of the Hall- and Nernst-type effects.

$$\boldsymbol{j}^{\uparrow} = -\hat{L}_0^{\uparrow}\boldsymbol{\nabla}\mu^{\uparrow} - \frac{1}{T}\hat{L}_1^{\uparrow}\boldsymbol{\nabla}T. \quad (2)$$

Here $\hat{L}_0^{\uparrow}$ and $\hat{L}_1^{\uparrow}$ are linear transport coefficients in a tensor form, $\mu^{\uparrow}$ denotes the chemical potential, and T is the sample averaged temperature. Thus, for the calculation of the spin current or spin accumulation, the linear transport coefficients

$$\hat{L}_n^{\uparrow}(T) = -\frac{1}{e}\int dE\hat{\sigma}^{\uparrow}(E)\left(-\frac{df_0(E,T)}{dE}\right)(E-\mu)^n \quad (3)$$

with $n = 0, 1$ are required. Here, $f_0(E, T)$ is the Fermi function and $e = |e|$ is the elementary charge. Obviously, the tensors $\hat{L}_n^{\uparrow}(T)$ have the same matrix structure as the conductivity tensor

$$\hat{\sigma}^{\uparrow} = \begin{pmatrix} \sigma_{xx}^{\uparrow} & -\sigma_{yx}^{\uparrow} & 0 \\ \sigma_{yx}^{\uparrow} & \sigma_{xx}^{\uparrow} & 0 \\ 0 & 0 & \sigma_{zz}^{\uparrow} \end{pmatrix} \quad (4)$$

that is valid for a cubic host system with the z direction as the global quantization axis for the relativistic spinors. Time and space inversion symmetry provide spin degeneracy and the following identities are fulfilled:

$$\sigma_{xx}^{\uparrow} = \sigma_{xx}^{\downarrow}, \qquad \sigma_{yx}^{\uparrow} = -\sigma_{yx}^{\downarrow}, \qquad \sigma_{zz}^{\uparrow} = \sigma_{zz}^{\downarrow}. \quad (5)$$

According to Eq. (3), the $\hat{\sigma}$ tensor has to be calculated as an energy-dependent quantity. Because of the strong decay of the energy derivative of $f_0(E, T)$, a small interval around the Fermi energy ($E_{\min} = E_F - 0.273$ eV $\leq E \leq E_F + 0.273$ eV $= E_{\max}$ with 57 energy points) is sufficient for the integration. An energy mesh, which is denser around E_F, and further interpolating points are used to improve the convergence.

We motivate our choice of Au, Ti, and Bi as substitutional atoms by the fact that their local density of states (LDOS) shows distinct features for different impurities (Fig. 2, upper panel). The impurity states are either below (Au) or above (Ti) the Fermi energy and the actual values for the LDOS differ by one order of magnitude at E_F. This should affect the linear transport coefficients significantly. A reason for the investigation of the Cu(Bi) alloy is the corresponding large spin Hall angle [19] that may provide a strong SNE as well.

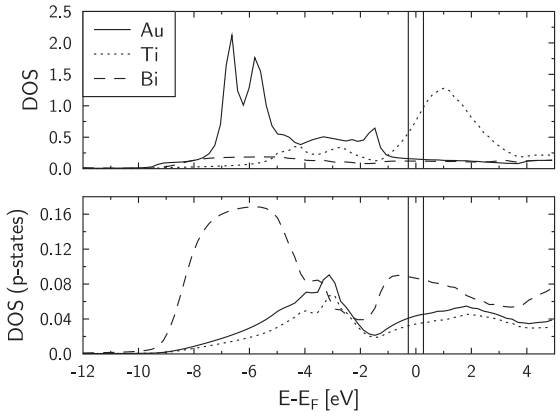

FIG. 2. Total LDOS for the Au, Ti, and Bi impurities in a Cu host (upper panel) and p states only (lower panel). The energy interval ($E_{\min}$, $E_{\max}$) is depicted by the vertical lines.

First of all, we present the calculated longitudinal and spin Hall conductivities for the three different impurities in Table I. Their energy dependence is nearly linear in the investigated interval. Therefore, for further analysis it is sufficient to know the conductivities at E_F and the differences $\Delta\hat{\sigma}^{\uparrow} = \hat{\sigma}^{\uparrow}(E_{\max}) - \hat{\sigma}^{\uparrow}(E_{\min})$, which are relevant for $\hat{L}_0^{\uparrow}$ and $\hat{L}_1^{\uparrow}$, respectively. For Cu(Au) and Cu(Bi) alloys the dominant contribution to $\sigma_{xx}^{\uparrow}$ is provided by p states, while d states dominate in the case of Cu(Ti) alloys. Taking into account that $\hat{\sigma} \propto \tau$, where the momentum relaxation time τ is inversely proportional to the impurity LDOS, the trend for $\sigma_{xx}^{\uparrow}(E_F)$ in Table I can be explained by considering the upper panel of Fig. 2 for Cu(Ti) and the lower panel for Cu(Au) and Cu(Bi) alloys. The sign of $\Delta\sigma_{xx}^{\uparrow}$ is provided by the slope of the corresponding curves of the partial LDOS. The quantities $\sigma_{yx}^{\uparrow}$ and $\Delta\sigma_{yx}^{\uparrow}$ cannot be explained in such a simple model since the spin Hall conductivity is caused by vertex corrections (scattering-in term) [18].

For our theoretical description we choose the temperature gradient ∇T in x direction, which will result in a spin current or spin accumulation along the y axis. At first we consider an electrically insulated system, where in equilibrium no currents are flowing. Under this condition we can rewrite Eq. (2) as

$$\frac{1}{e}\boldsymbol{\nabla}\mu^{\uparrow} = \hat{S}^{\uparrow}\boldsymbol{\nabla}T, \qquad \hat{S}^{\uparrow} = -\frac{1}{eT}\hat{L}_0^{\uparrow -1}\hat{L}_1^{\uparrow}, \quad (6)$$

where $\hat{S}^{\uparrow}$ is the thermopower and $\frac{1}{e}\boldsymbol{\nabla}\mu^{\uparrow}$ corresponds to the electric field provided by spin-up electrons. The resulting electric field

$$\boldsymbol{E} = \frac{1}{2}\frac{1}{e}(\boldsymbol{\nabla}\mu^{\uparrow} + \boldsymbol{\nabla}\mu^{\downarrow}) = \frac{1}{2}(\hat{S}^{\uparrow} + \hat{S}^{\downarrow})\boldsymbol{\nabla}T = \hat{S}\boldsymbol{\nabla}T \quad (7)$$

is connected with the temperature gradient via the total thermopower $\hat{S}$, which is given by the mean value of the thermopower for both relativistic spin channels. For the Seebeck effect the relevant quantity is

TABLE I. Longitudinal conductivity $\sigma_{xx}^{\uparrow}$ and spin Hall conductivity $\sigma_{yx}^{\uparrow}$ with their changes in units of $(\mu\Omega\,\mathrm{cm})^{-1}$ at an impurity concentration of 1 at. %. For comparison, the experimental residual conductivity $\sigma_{xx}^{\mathrm{exp}} = 2\sigma_{xx}^{\uparrow}$ is given [24].

Imp.	$\sigma_{xx}^{\mathrm{exp}}/2$	$\sigma_{xx}^{\uparrow}(E_F)$	$\sigma_{yx}^{\uparrow}(E_F)$	$\Delta\sigma_{xx}^{\uparrow}$	$\Delta\sigma_{yx}^{\uparrow}$
Au	0.96	1.32	1.33×10^{-2}	-1.94×10^{-2}	5.51×10^{-3}
Ti	0.06	0.04	1.62×10^{-4}	-1.93×10^{-2}	-1.64×10^{-4}
Bi	0.10	0.12	1.01×10^{-2}	1.18×10^{-2}	6.37×10^{-4}

$$S_{xx} = -\frac{1}{eT}\frac{(L^{\uparrow}_{0,xx}L^{\uparrow}_{1,xx} + L^{\uparrow}_{0,yx}L^{\uparrow}_{1,yx})}{{L^{\uparrow}_{0,xx}}^2 + {L^{\uparrow}_{0,yx}}^2}. \quad (8)$$

The electric field is induced only in x direction $E_x = S_{xx}\nabla_x T$ since the thermopower tensor is diagonal for nonmagnetic systems with cubic symmetry. Similarly, it is possible to define the spin Seebeck coefficient (SSC)

$$\frac{1}{2}\frac{1}{e}(\boldsymbol{\nabla}\mu^{\uparrow} - \boldsymbol{\nabla}\mu^{\downarrow}) = \frac{1}{2}(\hat{S}^{\uparrow} - \hat{S}^{\downarrow})\boldsymbol{\nabla}T = \hat{S}^{s}\boldsymbol{\nabla}T, \quad (9)$$

where its component

$$S^{s}_{yx} = -\frac{1}{eT}\frac{(L^{\uparrow}_{0,xx}L^{\uparrow}_{1,yx} - L^{\uparrow}_{0,yx}L^{\uparrow}_{1,xx})}{{L^{\uparrow}_{0,xx}}^2 + {L^{\uparrow}_{0,yx}}^2} \quad (10)$$

couples the temperature gradient with a spin accumulation in y direction $\frac{1}{2e}\nabla_y(\mu^{\uparrow} - \mu^{\downarrow}) = S^{s}_{yx}\nabla_x T$.

The obtained values of S_{xx} and S^{s}_{yx} for the three impurities in a Cu host are shown in Fig. 3. Both quantities are independent of the impurity concentration since all linear transport coefficients are inversely proportional to the impurity concentration in the limit of dilute alloys. For all the investigated systems the relations $|\sigma^{\uparrow}_{xx}\Delta\sigma^{\uparrow}_{xx}| \gg |\sigma^{\uparrow}_{yx}\Delta\sigma^{\uparrow}_{yx}|$ and $|\sigma^{\uparrow}_{xx}| \gg |\sigma^{\uparrow}_{yx}|$ are valid. Because of Eq. (3) this gives $S_{xx} \approx \tilde{S}_{xx} = -\frac{1}{eT}L^{\uparrow}_{1,xx}/L^{\uparrow}_{0,xx}$, where $\tilde{S}_{xx}$ is the thermopower for the short-circuit case presented below. The quantity $L^{\uparrow}_{1,xx}$ has the same order of magnitude for all three considered impurities. However, due to its high longitudinal residual conductivity, the Cu(Au) alloy has the smallest thermopower. Clearly, the sign of S_{xx} and

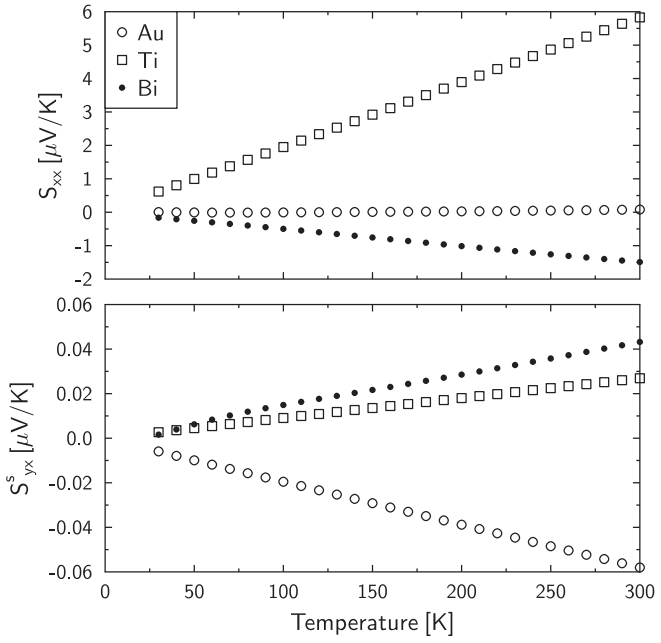

FIG. 3. A diagonal component of the thermopower (upper panel) and yx component of the spin Seebeck coefficient (lower panel) for a Cu host with Au, Ti, and Bi impurities.

therefore the direction of the induced electric field is determined by $\Delta\sigma^{\uparrow}_{xx}$ shown in Table I. In the lower panel of Fig. 3 we show $\hat{S}^{s}_{yx}$. In comparison to S_{xx}, this quantity has the same order of magnitude for Au and is two orders of magnitude smaller for Ti and Bi impurities. The sign of S^{s}_{yx} is more difficult to understand since it is given by the interplay of two contributions. To evaluate the strength of the SNE, one can use the spin Nernst angle $\beta = S^{s}_{yx}/S_{xx}$, which is an analogue to the spin Hall angle $\alpha = \sigma^{\uparrow}_{yx}/\sigma^{\uparrow}_{xx}$. At 300 K this ratio is equal to -0.72, 0.0046, and -0.029 for Au, Ti, and Bi impurities, respectively. For the Cu(Ti) and Cu(Bi) alloys β has the same order of magnitude as the corresponding α while for the Cu(Au) alloy its absolute value is about 70 times larger than α, which points to a more effective "conversion" of the longitudinal driving field into the transversal spin accumulation for this alloy.

Now we consider the short-circuit case in y direction, where the spin current is created instead of the spin accumulation. In x direction the system is still insulated with $j^{\uparrow}_x = j^{\downarrow}_x = 0$. In comparison to the SHE, where the spin current density is linearly proportional to the electric field via the spin Hall conductivity $\sigma_{yx} = j^{s}_y/E_x$, now we are interested in the relation between the temperature gradient and the spin current density

$$j^{s}_y = \sigma_{\mathrm{SN}}\nabla_x T. \quad (11)$$

Here we call the linear coefficient σ_{SN} spin Nernst conductivity (SNC) although it has not the units of a conventional conductivity. Replacing the x component of the electric field in the transverse spin current density [7]

$$j^{s}_y = -2eL^{\uparrow}_{0,yx}E_x - \frac{2}{T}L^{\uparrow}_{1,yx}\nabla_x T \quad (12)$$

by $E_x = \tilde{S}_{xx}\nabla_x T$ leads to

$$\sigma_{\mathrm{SN}} = \sigma^{E}_{\mathrm{SN}} + \sigma^{T}_{\mathrm{SN}} = -2e\tilde{S}_{xx}L^{\uparrow}_{0,yx} - \frac{2}{T}L^{\uparrow}_{1,yx}. \quad (13)$$

Taking into account the relations $L^{\uparrow}_{0,xx} \approx -\sigma^{\uparrow}_{xx}(E_F)/e$ and $|L^{\uparrow}_{0,xx}| \gg |L^{\uparrow}_{0,yx}|$, we can write

$$\sigma_{\mathrm{SN}} \approx -2\sigma^{\uparrow}_{xx}(E_F)S^{s}_{yx}, \quad (14)$$

which is a simple connection between the SNC and SSC.

It is interesting to discuss the two contributions to the SNC, defined in Eq. (13), separately. There, the term σ^{T}_{SN} gives the direct contribution from the temperature gradient. Additionally, the SNC is influenced by the SHE, which is present due to the electric field induced by the Seebeck effect. This contribution is given by σ^{E}_{SN}. Depending on the sign of the thermopower (Fig. 3), this term can be positive (Au, Ti) or negative (Bi) (Fig. 4) although the SHE has the same direction for all three impurities. The other term σ^{T}_{SN} has for the Cu(Ti) and Cu(Bi) alloys the same order of magnitude but the opposite sign in comparison to σ^{E}_{SN}. This leads to a partial compensation of both contributions

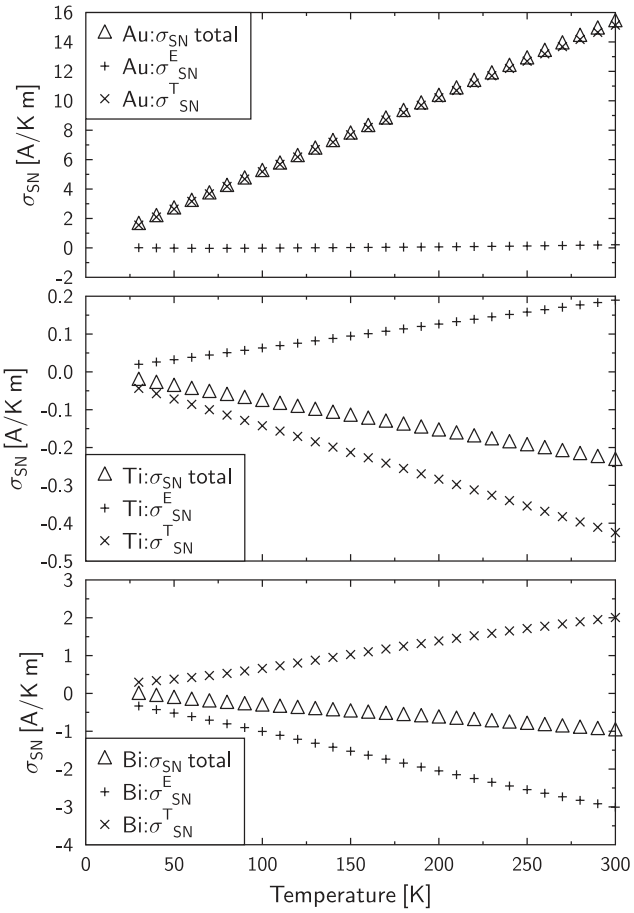

FIG. 4. Spin Nernst conductivity for Au (upper panel), Ti (middle panel), and Bi (lower panel) impurities in a Cu host at an impurity concentration of 1 at. %.

with reduced values of the total SNC. In contrast, for the Cu(Au) alloy the SNC is strongly dominated by σ^{T}_{SN} providing much higher values than for the other two alloys. On the other hand, S^{s}_{yx} is obtained to be of the same order of magnitude for all considered alloys. Thus, according to Eq. (14), the large values of σ_{SN} for the Cu(Au) alloy are simply caused by the high residual conductivity (see Table I). This is opposite to the SHE where for a pronounced effect one needs strong scattering [19,21].

In fact, the SNC depends on the impurity concentration. For comparison between different dilute alloys discussed in this Letter, we fixed the concentration at 1 at. %. Assuming a sample size of $100 \times 100 \times 100$ nm used typically in spin Hall devices [25] and the temperature gradient of 50 K/μm present in recent thermoelectric experiments [14], we estimate a spin current of about 10 μA in the Cu(Au) alloy at room temperature. Thus, a spin current of the order of 100 μA is reached with an impurity concentration of 0.1 at. %. This order of magnitude for the spin current is large enough to switch a nanomagnet as shown in recent experiments [26]. To obtain a comparable value considering the SHE for the same sample size and using $\alpha \sim 0.01$ for Cu(Au), a charge current density of $\sim 10^{12}$ A/m^2 is needed. This is close to the electromigration regime [14]. It means the application of both effects is experimentally comparably challenging. Of course, it is questionable to stabilize the assumed temperature gradient in copper, which is highly thermally conductive. However, even a spin current one or two orders of magnitude smaller than 100 μA would be detectable.

In our approach we neglected any phonon contributions. The spin Hall conductivity of a Cu(Ir) dilute alloy was found to be practically temperature independent [27]. This indicates that the impurity skew-scattering contribution, provided in our calculation by $L_{0,yx}$ and $L_{1,yx}$, dominates in a Cu host. The charge transport is however a superposition of impurity and phonon contributions. Experimental data for copper at room temperature are $\sigma_{xx} = 0.4(\mu\Omega\,\mathrm{cm})^{-1}$ and $S_{xx} = 1.6$ μV [14]. Comparing these values with our results, the deviations are strongest for the Cu(Au) alloy, for which we obtained $\sigma_{xx} = 2.64(\mu\Omega\,\mathrm{cm})^{-1}$ and $S_{xx} = 0.08$ μV/K. Using Eq. (13) with the experimental data we can estimate the SNC to be increased by 30% due to phonons. In contrast, the spin Nernst angle, calculated according to Eq. (14) as $\beta \approx -\sigma_{SN}/(\sigma_{xx}S_{xx})$, is changed from -0.72 to -0.28, keeping the same order of magnitude. Thus, an experimental observation of the SNE seems to be promising.

In summary, a first principle approach for the description of the skew-scattering contribution to the spin Nernst effect in dilute metallic alloys is presented. We calculated the thermopower, the transverse spin Seebeck coefficient, and the spin Nernst conductivity providing a linear relation between the transverse spin current and the temperature gradient. The amount and direction of the spin current can be tuned by different impurities. The spin currents, which are generated by either a temperature gradient or an external electric field, can flow in the same or in the opposite direction depending on the impurity. This means that the presence of a temperature gradient in spin Hall devices can be constructive or destructive. The large spin Nernst current, obtained at room temperature for the Cu(Au) alloy, makes this alloy attractive for experimental investigations.

This work was supported by the Deutsche Forschungsgemeinschaft (DFG) via SFB 762 and the priority program SSP 1538. In addition, M. G. acknowledges financial support from the DFG (GR3838/1-1).

*ktauber@mpi-halle.mpg.de

[1] M. I. Dyakonov and V. Perel, Phys. Lett. **35A**, 459 (1971).
[2] J. Hirsch, Phys. Rev. Lett. **83**, 1834 (1999).
[3] G. E. Bauer, A. H. MacDonald, and S. Maekawa, Solid State Commun. **150**, 459 (2010).
[4] S.-G. Cheng, Y. Xing, Q.-F. Sun, and X. C. Xie, Phys. Rev. B **78**, 045302 (2008).
[5] X. Liu and X. Xie, Solid State Commun. **150**, 471 (2010).

[6] T. Miyasato, N. Abe, T. Fujii, A. Asamitsu, S. Onoda, Y. Onose, N. Nagaosa, and Y. Tokura, Phys. Rev. Lett. **99**, 086602 (2007).
[7] Z. Ma, Solid State Commun. **150**, 510 (2010).
[8] K. Uchida, S. Takahashi, K. Harii, J. Ieda, W. Koshibae, K. Ando, S. Maekawa, and E. Saitoh, Nature (London) **455**, 778 (2008).
[9] K. Uchida, S. Takahashi, J. Ieda, K. Harii, K. Ikeda, W. Koshibae, S. Maekawa, and E. Saitoh, J. Appl. Phys. **105**, 07C908 (2009).
[10] K. Uchida *et al.*, Nature Mater. **9**, 894 (2010).
[11] C. M. Jaworski, J. Yang, S. Mack, D. D. Awschalom, J. P. Heremans, and R. C. Myers, Nature Mater. **9**, 898 (2010).
[12] J. Xiao, G. E. W. Bauer, K.-C. Uchida, E. Saitoh, and S. Maekawa, Phys. Rev. B **81**, 214418 (2010).
[13] S. Huang, W. G. Wang, S. F. Lee, J. Kwo, and C. L. Chien, Phys. Rev. Lett. **107**, 216604 (2011).
[14] A. Slachter, F. L. Bakker, J.-P. Adam , and B. J. van Wees, Nature Phys. **6**, 879 (2010).
[15] R. Jansen, A. M. Deac, H. Saito, and S. Yuasa, Phys. Rev. B **85**, 094401 (2012).
[16] M. Gradhand, M. Czerner, D. V. Fedorov, P. Zahn, B. Y. Yavorsky, L. Szunyogh, and I. Mertig, Phys. Rev. B **80**, 224413 (2009).
[17] I. Mertig, Rep. Prog. Phys. **62**, 237 (1999).
[18] M. Gradhand, D. V. Fedorov, P. Zahn, and I. Mertig, Phys. Rev. Lett. **104**, 186403 (2010).
[19] M. Gradhand, D. V. Fedorov, P. Zahn, and I. Mertig, Phys. Rev. B **81**, 245109 (2010).
[20] S. Lowitzer, M. Gradhand, D. Ködderitzsch, D. V. Fedorov, I. Mertig, and H. Ebert, Phys. Rev. Lett. **106**, 056601 (2011).
[21] M. Gradhand, D. V. Fedorov, P. Zahn, and I. Mertig, Solid State Phenom. **168–169**, 27 (2010).
[22] Y. K. Kato, R. C. Myers, A. C. Gossard, and D. D. Awschalom, Science **306**, 1910 (2004).
[23] J. Sinova, Nature Mater. **9**, 880 (2010).
[24] J. Bass, *Electrical Resistivity of Pure Metals and Alloys*, Landolt-Börnstein New Series, Group III, Part (a), Vol. 15 (Springer, New York, 1982).
[25] T. Kimura, Y. Otani, T. Sato, S. Takahashi, and S. Maekawa, Phys. Rev. Lett. **98**, 156601 (2007).
[26] T. Yang, T. Kimura, and Y. Otani, Nature Phys. **4**, 851 (2008).
[27] Y. Niimi, M. Morota, D. H. Wei, C. Deranlot, M. Basletic, A. Hamzic, A. Fert, and Y. Otani, Phys. Rev. Lett. **106**, 126601 (2011).